STRESS EVALUATION IN HIGH SPEED ROTATING MACHINERY WITH THE L_{CR} ULTRASONIC TECHNIQUE

by

Don E. Bray

Department of Mechanical Engineering

Texas A&M University

College Station, Texas

and

Martin Dietrich

Shop Services Manager

Sulzer Turbosystems International

LaPorte, Texas

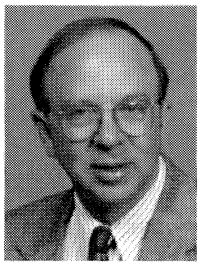

Don E. Bray is an Associate Professor of Mechanical Engineering at Texas A&M University in College Station, Texas. He has more than 30 years' experience in nondestructive evaluation and is a coauthor of a widely used textbook and a reference book on NDE. Prior to joining Texas A&M in 1978, he worked with the Southern Pacific Railway Company and the United States Department of Transportation.

Dr. Bray has a B.S. degree (Mechanical Engineering) from Southern Methodist University (1961), an M.S. degree (Mechanical Engineering) from the University of Houston (1969), and a Ph.D. degree from the University of Oklahoma (1977). He is a registered Professional Engineer in the States of Texas and Oklahoma, certified at Level III in ultrasonics by examination of the American Society for Nondestructive Testing, and holds fellow membership rank in both ASME and ASNT.

Martin Dietrich is Shop Services Manager for Sulzer Turbosystems International at the Sulzer owned turbomachinery repair facility Hickham Industries in LaPorte, Texas. He has 10 years' experience working on turbomachinery with Sulzer.

Mr. Dietrich has a B.S. degree (Mechanical Engineering) from the Swiss Engineering School in Burgdorf.

ABSTRACT

The L_{CR} ultrasonic technique is ideally suited for stress measurement, since it is a bulk longitudinal wave that propagates just underneath the surface of the item being inspected. Additionally, it is most sensitive to stress, and least sensitive to material texture. A description of the L_{CR} probe is included, and brief summaries are furnished of successful applications of the technique to stress evaluation in a turbine disk and a generator retaining ring. Additional discussion is given on an application to a compressor rotor that was found to be bowed. The measurements on the compressor rotor were conducted in an industrial shop, using readily available equipment. Only the probe was specially designed for the work. Discussions of other possible applications also are given.

INTRODUCTION

Manufacturing and service induced stresses play a key role in the satisfactory mechanical performance of high speed, rotating machinery. Dynamic and thermal stresses occur naturally due to operating characteristics. Design and maintenance engineers need to be aware of residual stresses, and try to eliminate them by a suitable stress relief method. Further, they must attempt to anticipate future changes in stress due to operations.

In all cases, the ability to measure these unknown, residual stresses has been limited, and the engineer has been required to take extra steps in the design, manufacture, and maintenance process to assure that they do not adversely affect performance. Problems of portability of the equipment and reliability of the data have led to limited nondestructive field measurement of stresses, however. With this, residual stress problems persist in mechanical systems. The present work is an attempt to develop a technique that offers the engineer residual stress information in a convenient and reliable format.

The following describes the application of an ultrasonic technique to stress evaluation in several components used in rotating equipment. An early application was to a generator retaining ring, where the prevailing stress field of a mounted ring was evaluated and found to be correctly distributed. Later, laboratory tests on a steam turbine disk showed an ability of the technique to measure stress changes induced by mechanical loads, and by section removal. Finally, a field application of the technique for evaluating stress conditions in a compressor rotor provided evidence that the rotor was bowed because of residual stresses. Future applications of the L_{CR} ultrasonic technique to rotating machinery components are discussed.

The L_{CR} ULTRASONIC TECHNIQUE

Ultrasonic techniques are regularly used for flaw detection in mechanical components and systems [1]. The technique involves a short stress wave pulse that is excited in the components with a piezoelectric transducer. The echo pattern of the pulse is used to evaluate any defects or other anomalous conditions in the part being inspected. Both normal beam and angle beam techniques are used. In the normal beam method, a longitudinal wave is usually excited at the surface, and travels in the part being inspected on a path normal to the surface. Angle beam techniques direct the ultrasonic energy to regions not reachable with the normal beam approach. Refraction at interfaces is governed by Snell's Law, as given by Equation (1). The L_{CR} technique is a special case of angle beam inspection, and is excited when the angle of incidence is slightly greater than the critically refracted angle, i.e., when θ_1' is just greater than 90 degrees. For the PMMA (Plexiglas®) and steel

combination (Figure 1), θ_1 will be 28 degrees and θ_2 will be 34 degrees.

$$\sin\frac{\theta_1}{C_1} = \frac{\sin\theta'_1}{C'_1} = \frac{\sin\theta'_2}{C'_2} \quad (1)$$

θ_1 is the angle of the incident longitudinal wave, and C_1 is the longitudinal wave speed in the incident material. Typical wave speeds for PMMA and steel are shown in Table 1. The primed components designate waves refracted in the material being inspected. The subscripts one and two designate longitudinal and shear waves, respectively.

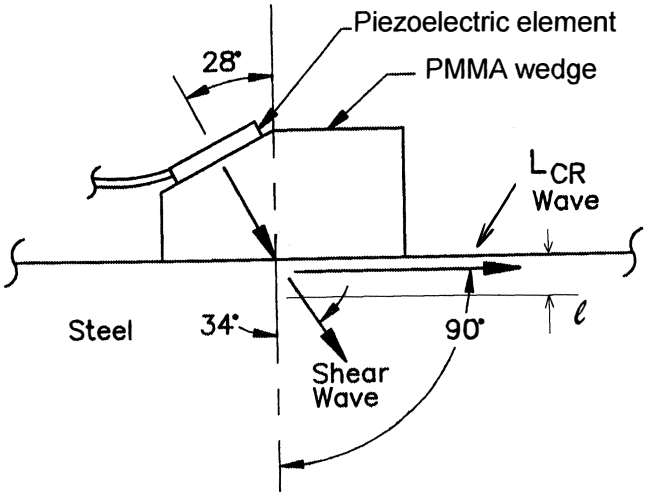

Figure 1. L_{CR} Probe for PMMA (Plexiglas®) on Steel.

Table 1. Longitudinal and Shear Wave Speeds in PMMA and Steel [1].

Material	C_1	C_2
	m/s	m/s
PMMA	2730	1430
Steel	5900	3230

The L_{CR} is a bulk longitudinal wave, traveling just below the surface of the specimen. The effective L_{CR} depth (ℓ), shown in Figure 1, is approximately equal to one wavelength (λ), as given by:

$$l = \lambda = \frac{C'_1}{f} \quad (2)$$

Where f is the probe frequency in Hz. Thus, this wave is sensitive to stress fields in a finite thickness and not just at the surface. Another important characteristic of this wave is that, in comparison to the shear waves, it is more sensitive to stress and, yet, less sensitive to localized material texture changes [1, 2]. Additional details on the angle beam L_{CR} probes and beam profiles are given by Junghans and Bray [3].

For stress measurement work, the L_{CR} probes are arranged in a tandem fashion (Figure 2), with one probe acting as the transmitter and the other as a receiver. Distance between the probes (d) is kept constant by the rigid space bar, assuring that any change in travel-time between the two probes is due to stress or material variations, and not a change in probe spacing. This design minimizes travel-time measurement errors that might occur due to transmitter triggering uncertainty, or wave speed changes in the transducers or wedges.

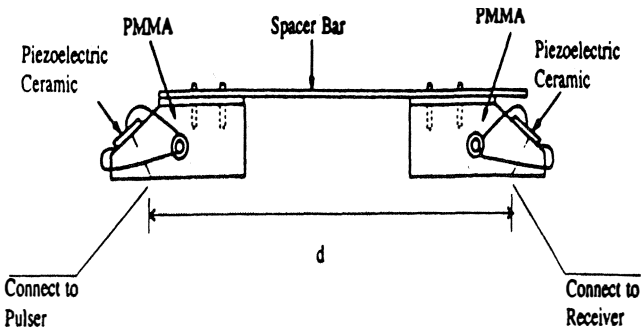

Figure 2. Typical Tandem L_{CR} Probe Arrangement Used for Stress Measurement.

To establish the presence of residual stresses in a member using L_{CR} waves, certain other parameters need to be considered. The effects of stress, texture, and temperature on the wave speed all contribute to the aggregate changes in data collected [4]. The relationship caused by such parameters may be expressed as:

$$t = t^* + \Delta t_{RS} + \Delta t_T + \Delta t_F + \Delta t_{TX} \quad (3)$$

Where t is measured travel-time, t^* is travel-time for a homogenous, isotropic, stressfree member at a standard temperature, Δt_{RS} is the travel-time effect of the residual stress, Δt_T is travel-time effect of the temperature difference at the time of measurement from the standard measurement, Δt_F is travel-time effect of an applied (active) force, and Δt_{TX} is travel-time effect of the material texture. For residual stress measurement, Δt_F can usually be assumed to be zero.

The relationship of measured L_{CR} wave travel-time change and the corresponding uniaxial stress is given by Egle and Bray [5] as:

$$\Delta\sigma = \frac{E}{Lt^*}(t - t^* - \Delta t_T) \quad (4)$$

where $\Delta\sigma$ is change in stress, E is Young's modulus, and L is the acoustoelastic constant for longitudinal waves propagating in the direction of the applied stress field. For assumed constant values of t^* and Δt_{TX} then, travel-time values (t) obtained at different locations on the rotor will indicate stress changes. Note that temperature variations may be established in the data set.

Previous applications of the technique have been for determining stress change in railroad rail and welded steel plate. Egle and Bray [5] showed that daily, temperature induced stress changes in a continuously welded railroad could be monitored with the L_{CR} method. Szelazek has used the method for evaluating thermally induced stresses in railroad rail [6]. Leon-Salamanca and Bray [7] and Bray and Junghans [8] showed that stress relieved welded plate could be differentiated from nonstress relieved plate based on L_{CR} data.

APPLICATIONS TO TURBINE AND COMPRESSOR COMPONENTS

Turbine Disk

A steel steam turbine disk used to evaluate the L_{CR} technique consisted of a bored hub, a connecting plate, rim, and blades [9]. The thickness of the hub and the rim measured 76.3 mm and 69.4 mm, respectively, and the disk outside diameter was 640 mm. The disk was abrasively blasted by the supplier for cleaning purposes prior to its receipt for investigation. The material composition was 0.56 percent C, 0.93 percent Mn, 0.011 percent P, 0.014 percent S, 0.27 percent Si, 0.03 percent Ni, 0.03 percent Cr, 0.03 percent Mo. Metallurgical analysis confirmed the composition of this material to be a normalized pearlitic steel. Hardness values measured at eight different locations around the faces of the inlet and outlet sides of the rim showed statistically significant differences in the

two sides. Tests using shear waves on samples cut from each side of the rim to indicate texture showed the material to be isotropic. Across the thickness of the hub, the longitudinal wave velocity measured with a normal beam 2.25 MHz, 12.7 mm diameter probe was found to be 5952 m/sec.

For the disk studies, tandem transducers, as shown in Figure 2, were used. Nominal probe frequency was 1.9 MHz and the spacing (d) was 109 mm (4.25 in). The effective depth (ℓ) would be approximately 3 mm (0.12 in).

To determine the residual stress in the initial state, two sections approximately 250 mm (10 in) long were cut from rim locations approximately opposite to each other. Strain gauges were installed before cutting, and L_{CR} travel-time data were measured in the sections before and after cutting. Section one was retained as a control specimen while section two was subjected to stress relief heat treatment.

The travel-time changes in the sections, due to removal by cutting from the disk, were −38.1 ns on the inlet side and +17.4 ns on the outlet side of the rim on the cut section one. For section two, travel-time changes due to the removal were much smaller, +3.5 and −6.7 ns, respectively. The travel-time pattern indicated that in the intact disk, the initial, uncut sections had stresses at the inlet face of section one and outlet face of section two that were more compressive before cutting. For the outlet side of section one and the inlet side of section two, the initial stresses were more tensile before cutting. Further experiments were conducted on section two using two stress relief heat treatments. The L_{CR} technique was again used to evaluate the residual stress in the section. To assure full stress relief, the same piece was again heat treated in a similar manner, except that it was held for an additional period of 10 hours. The L_{CR} technique then was used to determine the residual stress in the cut section. L_{CR} travel-time readings were taken on the inlet and outlet sides at both heat treatment stages. The average temperature corrected travel-times on the inlet and outlet side of the rims for the four-hour stress relief were 35.4181 μs and 35.3057 μs, respectively. After the additional 10 hour stress relief, the values were 35.4134 μs and 35.3126 μs. Stress change values resulting from the stress relief, calculated using Equation (4), are shown in Table 2.

Table 2. Stress Change Seen by L_{CR} Data for Section Two as Heat Treated MPa (ksi).

Condition	Inlet	Outlet
As-received	--	--
Stress relieved 10 hr.	275 (40)	–73.8 (–10.7)

The effects of the section removal and stress relief heat treatment were clearly indicated by the L_{CR} method. While there were slight disagreements between stress fields indicated by the L_{CR} and the strain gauge and X-ray diffraction methods used in conjunction with L_{CR}, these differences were felt to be due to the different stress fields being observed by the three techniques.

Turbine Retaining Ring

The holding quality of the shrink fit of generator retaining rings is dependent on the hoop residual stress in the ring, since the operating, centrifugal induced stresses will tend to release the retention force. Leon-Salamanca, et al. [10], describe an application of the L_{CR} technique in evaluating this stress, before and after mounting of the ring. The ring evaluated in this case measured 711 mm wide with a radius of 610 mm. The L_{CR} probe was situated so that travel-times were measured along a chord, in the hoop direction. Commercial, highly damped 2.25 MHz probes were used. Calibration was accomplished with a test sample cut from a spare retaining ring. Off the rotor, the travel-times in the ring were fairly uniform across its width. Fitted onto the generator, the travel-time pattern showed higher values at the outside, and minimum times at the center of the ring. The longer travel-times at the edges are indicative of more tensile stresses at the edge, and less tensile at the center. Specifications called for tensile stresses of 45 ksi at the edges, and 10 ksi at the center. The generally longer travel-times for the mounted *vs* unmounted position indicates the overall tensile effect of the ring being fitted on the generator. Stress change values cannot be estimated, since the probe spacing is not given.

Compressor Rotor

An evaluation of the residual stress at the inlet locations in the shaft using critically refracted longitudinal, L_{CR}, ultrasonic waves showed compressive stress on the bowed side of the rotor, supporting the conclusion that residual stress is the cause of the bow [11]. The seven stage compressor rotor was made of 34 Cr Ni Mo 6 steel, which is approximately a 4340 steel. It is just over three meters in length, with diameters of approximately 265 mm at the disk mounting areas (Figure 3). The location of each of the inlet stages is indicated by the number at the top of the rotor, above the arrows. Each of the compressor stages was mounted on the rotor at the time of the stress measurement. It had been run in service, and removed for normal maintenance, when the bow was observed. An almost continuous bow exists, with the maximum runout of 0.03 mm (0.0012 in) at the inlet to the fourth stage impeller. The fourth stage impeller is at the approximate middle of the rotor length. At the time that the data were taken, the rotor was horizontal, resting on two stands at the bearing faces indicated by the small triangles at each end.

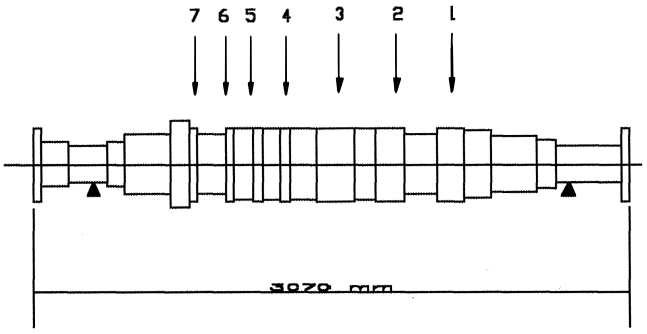

Figure 3. Diagram of Rotor Used for Ultrasonix Tests. (Inlet stage area indicated by number above arrows.)

In order to evaluate the contribution of residual stresses in the rotor, Δt_{RS} in Equation (3), contributions by the other parameters need to be considered. In the present case, only stress differences around the circumference are of importance, and a relatively constant t* for each data point is a reasonable assumption. While this assumption eliminates the possibility of defining quantitative stress values, qualitative analyses of stress change are still valid. Effects due to temperature changes are already well documented. Hence, by measuring the temperature along with the travel-time for each location, the contribution of Δt_T to overall t can easily be calculated. The effect of the weight of the rotor and disks, Δt_F, is of no consequence. The bending stress caused by these components was estimated to be approximately 3 MPa, which would result in a travel-time variation of 0.3 ns for the probe used. This value is small enough to be neglected. The effect of permanent deformation induced texture may be estimated from recently reported studies of a steel sample loaded in tension past the elastic limit [12]. The sample was loaded to a prescribed value past the load limit, and then the load was removed. Both the strain and the L_{CR} travel-time changes were recorded for each step, with no load. The results showed that at up to two percent permanent strain, the effect on travel-time appeared to be random at less than

1 ns. For the present rotor situation, a bent beam analysis using the 0.03 mm deviation given for the rotor shows the permanent strain to be approximately 3 $(10)^{-6}$. At this low strain, any effect of permanent deformation on the travel-time is expected to be inconsequential, considering the above conditions.

In order to effectively use L_{CR} waves for measurement of residual stress in a component, careful selections must be made regarding equipment and data collection processes. The instrumentation used for these tests is shown in Figure 4, and described as follows:

• *Equipment* —Equipment capable of exciting a stable L_{CR} wave and measuring small changes in ultrasonic travel-time is employed. The equipment used in this case (shown at the center of Figure 4) included the following:

• Oscilloscope: 4 Channel/400 MHz—0.01 ns accuracy in time-averaging mode

• Pulser/Receiver

• Probe, 2.25 MHz, 12.7 mm × 12.7 mm (0.500 in × 0.500 in) mounted on a modified commercial wedge

A typical L_{CR} arrival obtained on the rotor is shown in Figure 5. Arrival times of the L_{CR} wave are established by using the second, positive zero crossing of the arriving signal as the reference.

Figure 4. The Probe Calibration Sample and Clamp (Lower Left), Thermocouple Reader (Lower Middle), Oscilloscope (on Table) with Pulser/Receiver and Computer on Top.

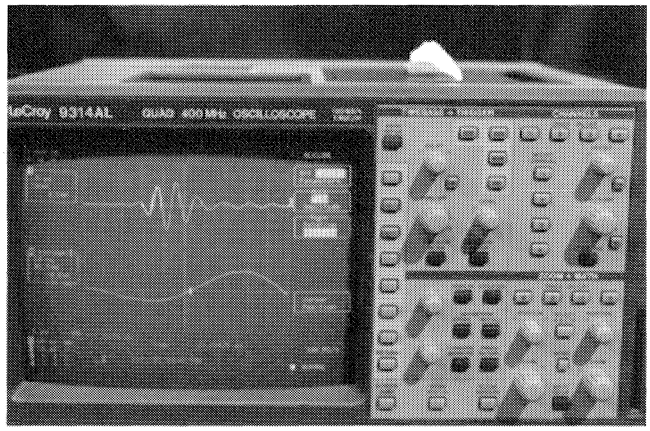

Figure 5. Oscilloscope Showing Typical Ultrasonic Signal.

• *Coupling Pressure*—Variations in pressure on the probes affects the travel-time. A uniform pressure is maintained with a probe designed especially for the rotor. The probe consisted of a typical tandem arrangement (Figure 2). It was secured to the rotor with a metal strip, screw type clamp fitted around the rotor circumference and over the probe. The probe at the left in Figure 4, and the screw clamp, are applied in a typical fashion over the calibration sample. Pressure adjustment on the probe was accomplished by tightening or loosening the screw on the circular clamp, while observing the amplitude of the pulse.

• *Systematic Errors*—Since the expected deviation in travel-time of the L_{CR} waves around the rotor may be less than 10 ns, it is essential that systematic errors be as small as possible. Measurement error is reduced significantly by using the constant pressure adjustment described above. Ultrasonic probe and instrumentation deviations in a known stressfree environment were established using a calibration test specimen, as shown in Figure 4. This specimen is made to represent the fourth stage area of the rotor in shape, size, and material. Travel-time data were taken on this test specimen, both in the laboratory and at the test site, in order to establish a generic ultrasonic test pattern for the material using the actual test setup. Repeated tests run on the calibration specimen were conducted and the instrumentation adjusted accordingly, until the deviation in the test data on this model specimen was limited to approximately two ns difference between locations around the calibration specimen. Calibrating the entire test setup in such a way ensured that the effect of extraneous parameters due to instrumentation were minimized in the actual test data.

The calibration specimen, probes, and instrumentation were transported to the repair shop where the actual shaft was being held (Figure 6). The rotor was marked circumferentially every 45 degrees between impellers three and four, four and five, and five and six from the inlet side. The probe in place on the rotor appears in Figure 7. Only one transducer is visible in the photograph; the opposite end of the probe assembly is hidden from view under the inlet stage of the impeller. Data on the calibration specimen and the shaft were collected on two different instances. For every position, multiple data points were taken to constitute a single data set for a particular location. A typical ultrasonic signal is shown in Figure 5.

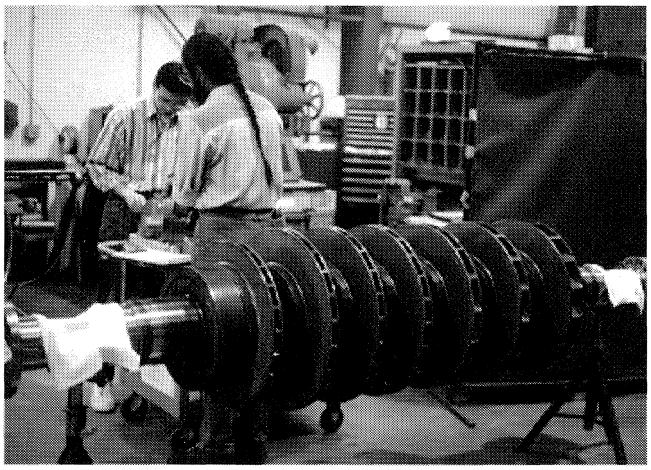

Figure 6. The Compressor Rotor. (Stage one is to the right, and the fluid flow is right to left.)

In the first test set (October 6 and 7, 1995), ultrasonic data sets were accumulated at each of the marked locations using two different probe sets. To minimize experimental error, data were taken using different test plans. The first data set was taken by keeping the probe set on the top and rotating the rotor by 45 degrees for each test location. Other variations included keeping the shaft stationary and moving the probes around the shaft to each location. Also, the sender and receiver probes were switched by 180 degrees for one data set. Data on the calibration block were

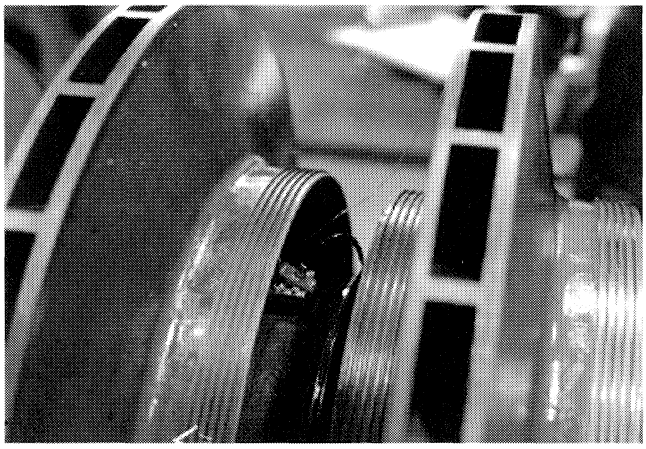

Figure 7. Probe in Place on the Rotor at Stage Four Inlet.

similarly collected. In the second test (October 21, 1995), all of the data sets were collected again for each test location.

Temperature data were obtained on both occasions. The rotor had been stored in a large, open shop building on the Texas Gulf Coast for a number of months through the summer. Temperature variations during a 24-hour period in this case are small. The probes were left in the open shop atmosphere to assure thermal equilibrium. For the first set (October 6 and 7, 1995) only atmospheric temperatures were taken. For the October 21, 1995 set, both atmospheric and probe temperatures were obtained. No significant differences were found between the probe and the atmospheric temperatures.

Travel-time data for the inlet to the fourth stage were obtained by first collecting six different sets of travel-time profiles at locations (θ) around the shaft, as described in the previous section. Each datum point is identified as $T_{i\theta}$, where i is the data set number (one through six) and θ is the location around the circumference. The data analyses proceeded as follows:

- A mean circumferential travel-time ($\overline{T_C}$) is calculated using all of the data.
- For each data point (i) at location θ, the deviation ($\Delta T_{i\theta}$) from the mean is calculated:

$$\Delta T_{i\theta} = T_{i\theta} - \overline{T_C} \tag{5}$$

- Finally, the mean deviation:

$$\overline{\Delta T_\theta} = \sum_{i=1}^{6} \frac{\Delta T_{i\theta}}{6} \tag{6}$$

is established for each circumferential location. These analyses reduced the random signal variations and, therefore, revealed more clearly the actual deviations in travel-time caused by the shaft.

Stress variations are estimated using the acoustoelastic constant for the material, Young's modulus, and the appropriate travel-times. The stress variations, shown in the last column, are plotted in the radar plot of Figure 8. For this material, the acoustoelastic constant value used in Equation (4) is 2.45, which is the same as for pearlitic steel. No serious disagreement caused by variations in the acoustoelastic constants between the materials is expected.

A zero value on the radar plot does not mean a zero stress level. This zero is a base line that is used to reference the travel-times around the shaft. The interpretation of the plot shows positive variations of approximately 34 MPa (+5 ksi) and 21 MPa (+3 ksi) at 90 degrees and 135 degrees, respectively. The zero degree and 315 degree locations also give positive stress values, just above 14 MPa (2 ksi). At 270 degrees, a −21 MPa (3 ksi) stress variation is seen. Thus, the maximum stress difference across the rotor is from

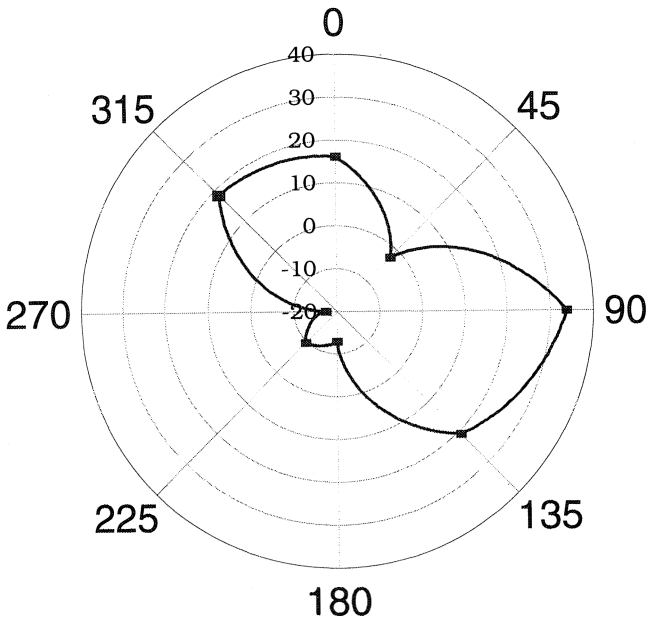

Figure 8. Stress Variations (in MPa) Around the Rotor at the Inlet to Stage Four.

the 90 degree to the 270 degree locations, and is almost 55 MPa (8 ksi).

Standard errors were calculated for each location. While the errors for some of the data were not small, statistical analyses showed that the data at the 90 degree and 270 degree locations are significantly different. The analysis of variances (ANOVA) results summarized in Table 3 supports statements about significant differences in experimental data. The analyses consider both the separation of the means, and the spread from the mean of the two data sets. For the ANOVA, an F value greater than F = 4.964591 is required for a 95 percent confident statement that the 90 degree and 270 degree data are different. The F = 5.949408 value clearly supports this statement.

Table 3. Single-Factor ANOVA of Travel-Time Deviations (ΔT_θ μs) at 90 Degree and 270 Degree Locations Around the Stage Four Inlet ($\alpha = 0.05$.)

	Location	
	90°	270°
	0.0012	-0.0012
	-0.0039	0.0007
	0.00485	-0.0001
	0.002475	0.005475
	0.006725	-0.002575
	0.013175	-0.003875
$\bar{x}$	0.004087	-0.002087
$\sigma_n^2 - 1$	0.000033	0.000005

$$F = 5.9494082 \quad F_{cr} = 4.9645905$$

Errors in the data may arise from three sources: the very small stress values being measured, the coupling of the probe, and the environmental noise in the industrial environment. While probe coupling was difficult in the confined space under the impeller

(Figure 7), measurable data were obtained. The effect of the industrial environment is demonstrated in the travel-times measured on their stress free calibration sample. In the laboratory at College Station, the variations around the sample were ±2 ns. In the turbine repair shop, the variations around the sample were ±5 ns. The source of these variations is not clear, but it may be the higher level of electromagnetic radiation in the industrial environment. Effects of temperature change were minimal, since temperatures stayed in the range of 24°C to 26°C (75.5°F to 78.6°F).

The travel-time deviations for the inlets to stages five and six showed patterns different from that seen for the inlet to stage four. For the inlet to stage six, the 315 degrees location showed an increase of 10 ns over the average, considerably larger than any value seen for the other stations. Other locations had deviations similar to that seen for stage four. For stage five, the deviations were lower than the stage four, but the pattern was more irregular. While the individuals conducting the tests felt comfortable about the data at these other two stages, there were some factors that might be affecting the data. First, the probes were specifically designed for the stage four inlet, which had a small difference in diameter and longitudinal spacing from the comparable dimensions at stages five and six. The fit for the other two stages might not be as good as for stage four. Also, due to the limited access in the areas where the probe is fitted, some unknown surface condition could be influencing the data. With these circumstances, it is difficult to express specific conclusions for the behavior seen at stages five and six, and further investigations would be needed to obtain data here with the same degree of confidence that is felt for the data at the stage four inlet.

OTHER POTENTIAL USES OF THE L_{CR} ULTRASONIC TECHNIQUE

There are many potential applications of the L_{CR} method for residual stress, beyond those discussed here. Candidates are as follows:

- Post heat treatment stress evaluation in welded or weld repaired components
- Evaluate stresses in components that may have experienced overspeed, particularly where work hardening may have occurred.
- Identify blades with tensile stresses in the leading edge, to reduce erosion.
- Assure proper fitting stresses on piping and pipe connections.

MEASUREMENT OF ABSOLUTE STRESSES

The measurement of absolute, rather than residual, stresses would be a significant addition to engineering technology. This is a difficult task, however, due to the myriad of factors that similarly affect the entire physical means that are used in stress measurement. Further, the zero stress condition is not easy to establish. For ultrasonics, for example, texture along with stress affects the wave speed. The measurement of a wave speed alone does not allow for the separation of residual and applied stresses, along with texture. The various ultrasonic methods used in stress measurement, and the techniques proposed for separating the different stresses, have been reviewed by Thompson, et al. [13]. The usefulness of measuring a quasiuniaxial stress field, which is the field measured by the L_{CR} method, is discussed by the authors.

FUTURE DEVELOPMENTS

The physics of using the L_{CR} method are apparently well established. Future developments of the method are very dependent on improved methods of data collection, along with better probe designs. To map a stress field requires a large amount of data, and the burdensome task of data collection and analysis limits the application, and increases the likelihood of measurement error. Further, uniform probe contact is the most serious error source in the data collection scheme. Obtaining good data requires extra care in probe positioning and pressure monitoring. Engineering improvements in the areas of data collection, analysis, and probe design will greatly facilitate the application of the method to new areas of stress measurement. With a concentrated effort, significant accomplishments toward these goals could be made in less than two years.

CONCLUSIONS

An ability to show the stress fields has been demonstrated for a limited number of applications to high speed, rotating equipment, using the L_{CR} technique. The turbine disk and generator retaining ring were simply used as demonstrations of the ability of the technique to measure stress change under well defined conditions. These tests succeeded. Additional work to build a database for application to other disk and retaining ring shapes and materials is needed for more general applications. For the rotor, an actual stress field was evaluated, and results consistent with the observed bow were confirmed. Stress studies using the L_{CR} method under actual bending conditions could improve the knowledge base on applying the technique.

At this point, it appears that the physical and material basis of the L_{CR} technique is well proved. Further development should center on the probe system and the data gathering and analysis system, along with developing a data base for application to more materials. At the present, each application requires a special probe design. Recent developments in composite, PVDF transducers may lead to the design of a probe that could be more universally applicable to rotating machinery components. Further, the integration of travel-time (i.e., stress) data into an overall data collecting scheme for the components will enhance the decision making process. The development of software to accomplish this is a desirable goal.

NOMENCLATURE

Residual stresses	=	Internal stresses contained in a body when all external constraints and forces are removed
Applied stresses	=	External stresses in a body due to being fitted into a larger assembly
L_{CR} method	=	Ultrasonic technique using critically refracted, bulk longitudinal waves
Snell's Law	=	Relationship of the incident, reflected, and refracted angles of waves at an interface
C_1, C_2	=	Bulk longitudinal and shear wave speeds, respectively
Probe assembly	=	A single unit containing an ultrasonic transducer and wedges for angle beam inspection
PMMA	=	Polymethyl methacrylate, clear organic glass used for making ultrasonic wedges, known by various trade names such as Plexiglas®, Lucite®, Perspex®
Acoustoelastic constant (L)	=	Elastic constant describing the relationship of strain and wave speed in a material
Coupling pressure	=	Pressure of the fluid couplant between the probe assembly and the part being studied

REFERENCES

1. Bray, D. E and Stanley, R. K., *Nondestructive Evaluation*, Revised Edition, Boca Raton, Florida: CRC Press (1997).
2. Egle, D. M. and Bray, D. E., "Measurement of Acoustoelastic and Third-Order Elastic Constants for Rail Steel," Journal of Acoustical Society of America, *60* (3), pp. 741-744 (1976).
3. Junghans, P. G. and Bray, D. E., "Beam Characteristics of High Angle Longitudinal Wave Probes," *NDE: Applications, Advanced Methods and Codes and Standards*, Eds. R. N. Pangborn *et al.*, PVP *216*, NDE *9*, Proceedings of the 1991 Pressure Vessels and Piping Conference, San Diego, California, (June 23-27, 1991), also, The American Society of Mechanical Engineers, New York, New York, pp. 39-44 (1991).
4. Bray, D. E. and Leon-Salamanca, T., "Zero-Force Travel-Time Parameters for Ultrasonic Head-Waves in Railroad Rail," Materials Evaluation, *43* (7), pp. 854-858, 863 (1985).
5. Egle, D. M. and Bray, D. E., "Application of the Acousto-Elastic Effect to Rail Stress Measurement," Materials Evaluation, *37* (4), pp. 41-46, 55 (1979).
6. Szelazek, J., "Ultrasonic Measurement of Thermal Stresses in Continuously Welded Rail," NDT&E International, *25* (2), pp. 77-85 (1992).
7. Leon-Salamanca, T. and Bray, D. E., "Residual Stress Measurements in Steel Plates and Welds Using Critically Refracted (L_{CR}) Waves," Research in Nondestructive Evaluation, *7* (4), pp. 169-184 (1996).
8. Bray, D. E. and Junghans, P.G., "Applications of the L_{CR} Ultrasonic Technique for Evaluation of PostWeld Heat Treatment in Steel Plates," NDT&E International, *28* (4), pp. 235-242 (1995).
9. Bray, D. E., Pathak, N., and Srinivasan, M. N., "Residual Stress Mapping in a Steam Turbine Disk Using the L_{CR} Ultrasonic Technique," Materials Evaluation, *54* (7), pp. 832-839 (1996).
10. Leon-Salamanca, T., Reinhart, E., Bray, D. E., and Golis, M., "Field Applications of an Ultrasonic Method for Stress Measurement in Structure," in Boogaard, J. and Van Dijk, G., Eds., *Nondestructive Testing (Proceedings Twelfth World Conference)*, Amsterdam, The Netherlands, pp. 1484-1489 (April 1989).
11. Bray, D. E., Tang, W., and Grewal, D., "Ultrasonic Stress Evaluation in a Turbine/Compressor Rotor," to appear, Journal of Testing and Evaluation (September 1997).
12. Tang, W. and Bray, D. E., "Stress and Yielding Studies Using Critically Refracted Longitudinal Waves," *NDE Engineering Codes and Standards and Material Characterization, Proceedings 1996 ASME Pressure Vessels Piping Conference*, Montreal, Quebec (July 1996), also, PVP *322*, NDE *15*, J. F. Cook, Sr., C. D. Cowfer, and C. C. Monahan, Eds. The American Society of Mechanical Engineers, New York, New York, pp. 41-48 (1996).
13. Thompson, R. B., Lu, W. Y., and Clark, Jr., A. V., "Ultrasonic Methods," Chapter 7, in *Handbook of Measurement of Residual Stress,* Lu, J., James, M., and Roy, G., Eds., Society for Experimental Stress Analysis, Bethel, Connecticut, pp. 149-178 (1996).

ACKNOWLEDGEMENT

The projects reported here were conducted with contributions and support from a variety of sources. These are cited in the individual original descriptions of the work.